

1 12

2 **Variability, Noise, and Sensitivity to**
3 **Error in Learning a Motor Task**

AU: Please check all mathematics and equations carefully for missing/dropped characters, etc.

4 DAGMAR STERNAD AND MASAKI O. ABE

5 When trying to understand human motor control probably the most funda-
6 mental aspect to consider is that the neuromechanical system is redundant.
7 A task as trivial as inserting a key into a keyhole can be successfully
8 achieved with the key approaching from a range of different orientations.
9 Biomechanical analysis of the multisegmented arm and hand pointing the
10 key immediately reveals that even for a single key orientation, an infinite
11 set of joint configurations exists. Redundancy also exists at the level of
12 muscles, such that many different muscle contractions will achieve the
13 same joint orientation. In fact, redundancy resides across all levels of the
14 neuromechanical system ranging from molecular, neuronal, and muscular,
15 to behavioral processes (see also Herzog, this volume). With this multiplic-
16 ity of options to achieve a given task, it is no surprise that variability at the
17 behavioral level is ubiquitous.

18 Variability at the task level is also the inevitable product of multiple
19 sources of noise in the nervous system.¹ For example, it has been shown that
20 noise arises in signal propagation due to synaptic fluctuations that increases
21 the irregularity of spike trains; in muscles and proprioceptors unavoidable
22 variations are added by the transduction between a continuous signal into

¹ A notational clarification on noise and variability: Although these terms are often difficult to keep apart, we distinguish between them as follows: *Variability* is the behavioral outcome of such system-intrinsic noise; capitalized *Noise* is one of the three concepts of the TCN approach and refers to the stochastic component that is assumed to be the result of intrinsic neuromotor noise; *N-Cost* is the operationalization of *Noise*. *Intrinsic (neuromotor) noise* refers to system-intrinsic fluctuations that are typically unwanted but from our perspective may also be fundamental to adaptation and control.

1 discrete spike sequences (Faisal et al. 2008). Noise also occurs at all stages
2 of the sensorimotor sequence, from the planning stage (Gordon et al. 1994;
3 Churchland et al. 2006), to the execution of movements (van Beers et al.
4 2004; van Beers 2009), and to the processing of sensory estimates to update
5 motor commands (Osborne et al. 2005) to the interaction with objects in a
6 variable environment. This noise, or uncertainty, is also an integral element
7 of current Bayesian approaches and has become the object of much theoriz-
8 ing and empirical work on perception, cognition, and motor control (van
9 Beers et al. 2002; Körding et al. 2004; Körding and Wolpert 2004; Miyazaki
10 et al. 2005).

11 Taken together, task redundancy and system noise, it is no surprise that
12 sensorimotor performance varies with every new attempt. And yet, the
13 nervous system does not randomly vary its performance to achieve the
14 task goal. The hypothesis of our research is that the nervous system seeks
15 strategies that best accommodate for errors and noise; that is, it seeks solu-
16 tions with stability or robustness. How is such stable coordination learned?
17 Our research provides evidence that the central nervous system (CNS) is
18 aware of its intrinsic noise and recognizes solutions that are robust to noise.
19 In addition, the CNS utilizes this noise to locate the most error-tolerant
20 solutions. Although several lines of investigation pursue similar directions,
21 our approach is unique in postulating three conceptually different routes
22 to performance improvement and stability.

23 **Stability: Tolerance to Noise**

24 Defined broadly, stable solutions are those that tolerate errors without
25 negative effects on task performance and without requiring explicit correc-
26 tions. In a continuous dynamical system, stable solutions are those that
27 quickly recover from small perturbations (Strogatz 1994). Viewing noise as
28 a barrage of small perturbations, more stable solutions are also more toler-
29 ant of noise. Using the frequently used image of a ball in a potential well,
30 stability is high when the well is deep and steep (Fig. 12.1A). Stability of a
31 system can be probed by administering small perturbations and observing
32 how long it takes for the system to return to the stationary state (lowest
33 point in the well). Importantly, variability is the consequence both of the
34 steepness of the well (stability) and of the noise level. Hence, in a coordina-
35 tive system, increasing stability offers a “smart” solution, as return back to
36 steady state can happen without explicit error correction. The relevance of
37 dynamic stability to skilled performance has been demonstrated in our
38 previous research on rhythmically bouncing a ball (Wei et al. 2007; 2008).

39 A slightly different perspective on stability is required when consider-
40 ing a discrete system, such as a set of individual throwing actions; only
41 discrete estimates of each throw are considered, and nothing is known
42 about their time sequence. Unlike in continuous tasks, there is no direct

Q: Please check, shortening of RH is OK here?

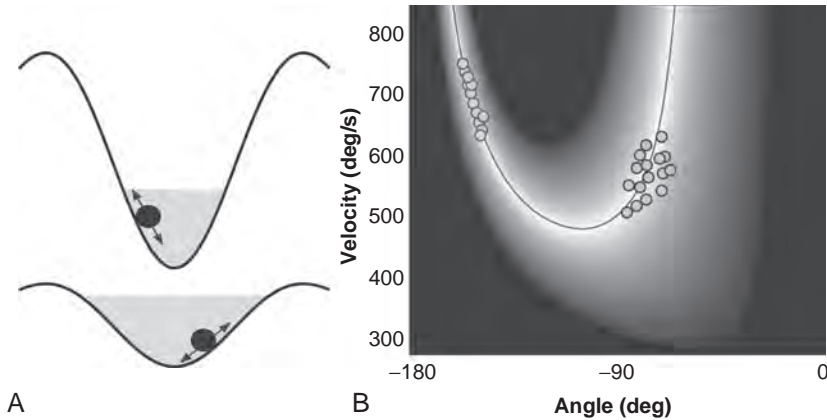


Figure 12.1 **A:** Stability and noise in a continuous dynamical system. The steepness of the well represents the stability of the system and the gray “filling” of the well represents the noise; the vertical level of the filling represents the effect of the variability. **B:** Discrete system with results as a function of two execution variables. The line denotes the zero-error solution manifold, darker shades denote increasing error. The two data sets exemplify how a location with shallow curvature adjacent to the solution manifold allows more noise or scatter in the data while still achieving comparable results than the data on the left.

1 carry-over of errors from the previous iteration and hence the concept of
 2 dynamical stability from dynamical systems theory cannot be applied “as
 3 is.” Figure 12.1B schematizes such a system using our model task of target-
 4 oriented throwing: Two variables, angle α and velocity v at ball release
 5 fully determine the trajectory of the projectile and its hitting accuracy or,
 6 generally, the result: $r = f(\alpha, v)$. In the figure, every throw is characterized
 7 by one data point of (α, v) with its associated result r shown by gray shades.
 8 The task is redundant, as many combinations of α and v achieve the same
 9 outcome r (e.g., hitting accuracy or error r). The U-shaped line denotes the
 10 desired zero-error solutions, $r = 0$, that define the solution manifold.
 11 The discrete system is said to be stable when a set of performances have
 12 the same or similar results r , even though the variables α and v may
 13 vary. As in the continuous system, stability of the discrete system is
 14 assessed by considering the effect of small perturbations. In the example
 15 of Figure 12.1B, the set of data on the right is more stable or more tolerant
 16 to error as the result function is shallower around the solution manifold
 17 than on the left: small perturbations to performance on the left will lead to
 18 large increases in error.

1 Tolerance, Covariation, and Noise Reduction

2 How does the sensorimotor system deal with its intrinsic noise and per-
3 form a redundant task with stability? We propose three routes to obtain
4 task stability (Fig. 12.2):

- 5 1. *Tolerance (T)*: The sensorimotor system seeks solutions that have
6 low sensitivity or high tolerance to errors. In nonlinear dynamical
7 systems this corresponds to seeking attractor states with steep
8 wells (Fig. 12.1A); in discrete systems this implies seeking loca-
9 tions on the manifold with a shallow curvature, such that small
10 deviations in α and v have minimal effect on the result.
- 11 2. *Covariation (C)*: Given the presence of intrinsic neuromotor noise,
12 the sensorimotor system develops covariation among variables
13 with respect to the solution manifold, such that a given amount of
14 noise has least effect on the result.
- 15 3. *Reduction of Noise (N)*: The sensorimotor system reduces the
16 magnitude of dispersion.

17 Figure 12.3 illustrates these three routes with schematic data plotted in
18 the execution space. Color shades code the result for data with different
19 release angle and velocities; white denotes zero error, the solution mani-
20 fold. Although each solution on the manifold is equivalent, different loca-
21 tions on the solution manifold have very different sensitivity or tolerance
22 to errors, as illustrated by the changing width of the light gray shades
23 adjacent to the solution manifold. The three panels contrast two data sets
24 respectively. One data set is ideal with respect to the three components: In
25 the left panel the two data sets have very different tolerance; the center
26 panel illustrates how data can covary to optimize the result; the right panel
27 illustrates how noise can be reduced.

28 We exemplify this three-pronged TCN approach by investigating a
29 throwing task to demonstrate that this framework can uncover processes

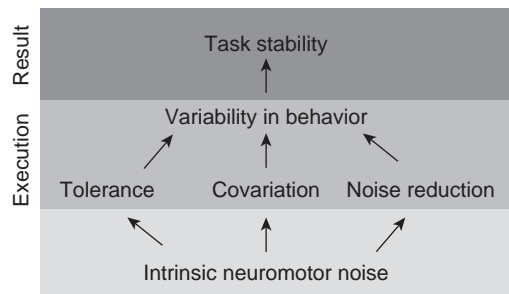


Figure 12.2 Schematic overview of the Tolerance, Covariance, Noise (TCN) approach.

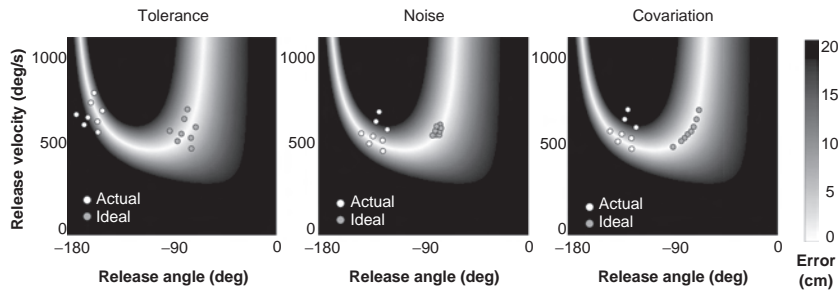


Figure 12.3 Three types of “costs” for motor variability. Actual (*white*) and ideal (*gray*) data optimized for Tolerance (*T-Cost*), and Noise (*N-Cost*), and Covariation (*C-Cost*).

- 1 underlying skill improvement and learning. Specifically, we show how the
- 2 three components are intertwined and how the brain uses variability to its
- 3 advantage.

4 Related Approaches

5 The notion of *constraining* or *channeling* the variability such that it has little
 6 effect on the result is also a core feature in the *uncontrolled manifold* (UCM)
 7 framework (Scholz and Schönner 1999; Latash 2008; see Latash, this volume).
 8 Central to the UCM approach is the tenet that control is indicated when
 9 over-repeated performances the system’s variability at the execution level
 10 shows anisotropic distribution in directions that do not affect the result
 11 (i.e., covary; Fig. 12.3B). Although the notions of reducing and channeling
 12 noise are conceptually consistent with the TCN-framework, UCM uses
 13 established mathematical tools of covariance analysis to quantify the aniso-
 14 tropic distribution of sets of data (Craig 1986; Latash 2008). Although this
 15 affords theoretical advantages, there are also disadvantages that will be
 16 considered in the discussion (Sternad et al., 2010). A second approach that
 17 has some conceptual overlap with the TNC method is the *optimal feedback*
 18 *control* (OFC) framework as developed by Todorov and colleagues (Todorov
 19 2004; Todorov 2005; see also Herzog, this volume). Extending traditional
 20 feedback control to delayed sensory estimates, OFC proposes a hierarchical
 21 control framework that applies selective control of task variables according
 22 to composite task-specific cost functions. Effectively, corrections are only
 23 applied when deviations have a devastating effect on the task goal, in the
 24 spirit of Gel’fand’s minimal intervention principle (Gel’fand and Tsetlin
 25 1962; Liu and Todorov 2007). Before elaborating on theoretical differences
 26 and possible insights derived from these different approaches, we review
 27 some recent research in our lab on the throwing task skillles.

AQ? In the refs, there are 2 Sternad et als, “submitted” and “accepted” please confirm which is correct here.

1 THE EXPERIMENTAL TASK

2 A throwing task called skittles has served as a test bed for our hypotheses.
3 In this task, subjects throw a ball suspended from a vertical post to hit a
4 target skittle that is located on the other side of the post. To execute an
5 accurate (not necessarily far) throw, subtle demands on the timing of ball
6 release have to be mastered. While the arm/hand trajectory prepares for
7 the throw (~250 ms duration), the final accuracy of the throw is solely
8 determined at the instant of release. Empirical and simulation-based
9 studies reported that the timing window for accurate throws is as short as
10 3–10 ms (Hore et al. 2002). This precision is astonishing, as a relatively
11 narrow range of covarying release variables is required at the instant of
12 release. Given these demands, the task has received considerable attention
13 in both sports- and clinically motivated research. For example, several
14 studies with cerebellar patients highlighted the significant involvement of
15 the cerebellum for the coordination between the continuous trajectory and
16 the precise timing of the release (Martin et al. 2001; Timmann et al. 2001;
17 Hore et al. 2002).

18 Apparatus and Data Collection

19 The experimental version of our skittles task reduced the movement to a
20 single-joint forearm rotation in the horizontal plane, where the ball release
21 is triggered via opening a contact switch by extending the index finger
22 during the forearm movement to simulate the throw of the ball (Fig. 12.4A).
23 The subject grasps a ball at the tip of the lever that has a contact switch
24 affixed. This switch can be closed by touch with the flexed index finger;
25 opening the contact by finger extension triggers ball release. The release
26 time determines the angular position α and angular velocity v of the arm
27 movement from which the ball trajectory is computed. This ball traverses
28 around the central post in an elliptic trajectory toward the skittle at the
29 opposite side (Fig. 12.4B). The subject sees this ball trajectory online on the
30 screen. The real arm movements with the manipulandum correspond to
31 paddle movements on the visual display that is seen by subjects as a bar
32 rotating around an axis. Angular displacements of the lever arm are
33 measured by a potentiometer. The virtual task is novel to every subject,
34 such that every learner has the same initial conditions. The task is simple
35 enough to allow improvement within the experimental time frame, but it
36 also provides sufficient subtleties that are only mastered with long-term
37 practice.

38 The ball's elliptic trajectories are generated by a two-dimensional model,
39 where two orthogonal springs attach the ball to the origin of the coordinate
40 system, the center post ($x = y = 0$). Due to restoring forces proportional to
41 the distance between ball and center post, the ball is accelerated toward the

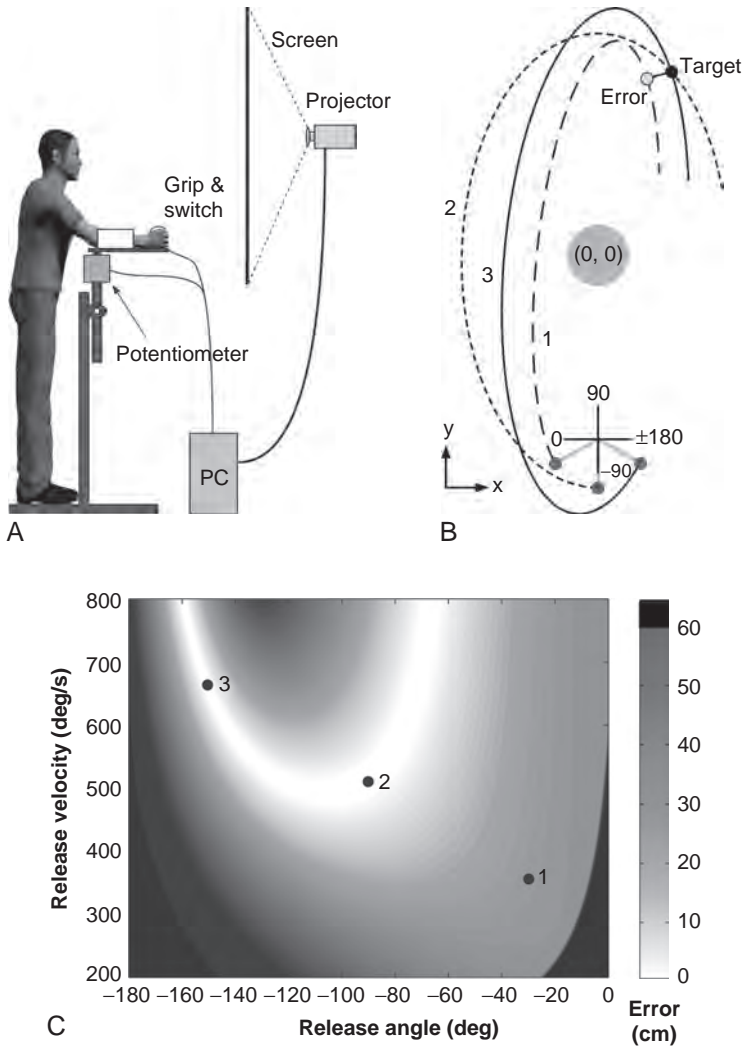


Figure 12.4 **A**: Experimental setup. Participants stand in front of the setup with their forearm resting on the horizontal lever arm. Rotation of the arm is recorded by a potentiometer; when the finger on the ball extends the contact switch opens and the ball in the virtual simulation is released. Online recordings of the arm movements are displayed on the projection screen. **B**: Three exemplary throws in workspace as participants see in the experiment. The view is a top-down view onto the pendular skittles task.

1 center. At time t , the equations for the ball position in x - and y - direction
2 are:

$$3 \quad x(t) = A_x \sin(\omega t + \varphi_x) e^{-\frac{t}{\tau}} \quad y(t) = A_y \sin(\omega t + \varphi_y) e^{-\frac{t}{\tau}} \quad (\text{Eq. 1})$$

4 The amplitudes A_x and A_y , as well as phase differences, φ_x and φ_y
5 result from the ball's release angle and velocity including energy conserva-
6 tion. The motions are lightly damped to approximate realistic behavior.
7 τ denotes the relaxation time of the decay. Figure 12.4B illustrates the defi-
8 nitions of the Cartesian coordinates of the workspace. Three exemplary ball
9 trajectories are displayed together with the result measure, d , defined as
10 the minimal distance between target and trajectory. The visual display is
11 shown to subjects on a back-projection screen that is placed at 1.2 m distant
12 from the subject.

13 The execution space with three data points corresponding to the three
14 trajectories is shown in Figure 12.4C. The result space and the solution man-
15 ifold are those used for the following experiment. Note that different target
16 locations render very different result functions (e.g., compare Figure 12.3
17 and 12.4C). Although each solution on the manifold is equivalent, different
18 locations on the solution manifold have very different sensitivity or toler-
19 ance to errors, as illustrated by the changing width of the light gray shades
20 adjacent to the solution manifold.

21 *General Procedure*

22 Each subject is presented the target position and is instructed to hit the
23 target skittle with the ball in its first elliptic trajectory. In all experiments,
24 the subjects execute their throws in a self-paced manner. Experience has
25 shown that they can perform 300 trials within one experimental session
26 without inducing fatigue or losing motivation and attention. The total
27 duration for 300 trials is approximately 30 minutes. For each trial, the exe-
28 cution variables release angle and the release velocity are measured, and
29 the elliptic trajectory of the ball is calculated and displayed. The result
30 measure, d , is calculated for each trial.

31 *TCN-Cost Analysis*

32 Cohen and Sternad (2009) adopted an optimization perspective to quantify
33 the three components (Cohen and Sternad 2009). Instead of calculating the
34 difference in T , C , and N between two data sets, as developed in Müller and
35 Sternad (2004), the new cost-based approach compares a single data set
36 with one that is optimized in one component, keeping others constant.
37 Note that the conceptual basis is unchanged, only the quantification is dif-
38 ferent. For a given data set, a virtual data set is numerically found that
39 optimizes T , N , and C (see Figure 12.3 for schematic illustration): Starting
40 with T , the actual data set is shifted across every location in execution space
41 in a grid-like manner without changing its relative distribution; at each

AQ? Müller and Sternad (2004) is not in refs...there is a 2009? Please check.

1 shift, its result is evaluated in terms of its average error; the best location in
 2 execution space is the one with the smallest error. The difference between
 3 the error of the actual and the best data set defines the cost due to non-
 4 optimal tolerance, *T-Cost*. To determine the cost due to nonoptimal covari-
 5 ation, *C-Cost*, the pairing of the two execution variables of a data set is
 6 permuted to find that combination of execution variables that achieves the
 7 best possible average result. *C-Cost* is the difference between the actual and
 8 the optimal result. Last, *N-Cost* is calculated by shrinking the data set con-
 9 centrically to its mean in n steps (e.g., $n = 100$). For each step, the result is
 10 evaluated and the best shrinking step is identified. Note the best result is
 11 not necessarily the single mean point, as it depends on the location. *N-Cost*
 12 is the difference in result between the initial set and the ideal one (for more
 13 details, see Cohen and Sternad 2009).

14 **Stages of Learning: From Exploration to Increasing Covariation** 15 **and Reducing Noise**

16 What insights can this analysis yield? Are all three components decreased
 17 by the same amount with practice, or is there a component that is
 18 inaccessible to optimization? Is there a specific sequence to how the three
 19 components are optimized? What does fine-tuning of a skill imply? To
 20 address these questions, a group of 12 healthy adult subjects practiced the
 21 skittles task for six experimental sessions on 6 days. Three additional par-
 22 ticipants who had extensive previous experience with throwing continued
 23 practice for a total of 15 days; two of them were intramural Frisbee players
 24 and one was a former professional cricket player. On each day, participants
 25 completed three blocks of 60 throws, leading to a total of 1,080 throws for
 26 the normal group and 2,700 throws for the expert subjects. The goal of the
 27 long-term data collection was to examine how accurate and precise human
 28 subjects can become in this task.

29 A first inspection of the average error and its standard deviations per
 30 block for each participant over practice showed the expected exponential
 31 decrease of the error and also of its standard deviations (Fig. 12.5). These
 32 results are consistent with many previous reports on performance improve-
 33 ments with practice (Schmidt and Lee 2005) and therefore can be seen as a
 34 representative database for examining the changes in the three components
 35 *Tolerance*, *Covariation*, and *Noise*.

36 Figure 12.6 shows the data of one of the expert subjects plotted in execu-
 37 tion space. As can be seen, on Day 1, the 60 data points of one block show
 38 a wide scatter, with most throws at larger release angles of -150 degrees.
 39 The fewer throws with a release angle around -80 degrees were later in the
 40 block, "exploring" other areas of execution space to achieve better perfor-
 41 mance in with executions that are more error-tolerant (trial sequence in time
 42 is not visible in the figure). On Day 5, this location in execution space evi-
 43 dently became preferred, and the data start to cluster with some *Covariation*
 44 along the solution manifold. On Day 15 of practice, the data have become

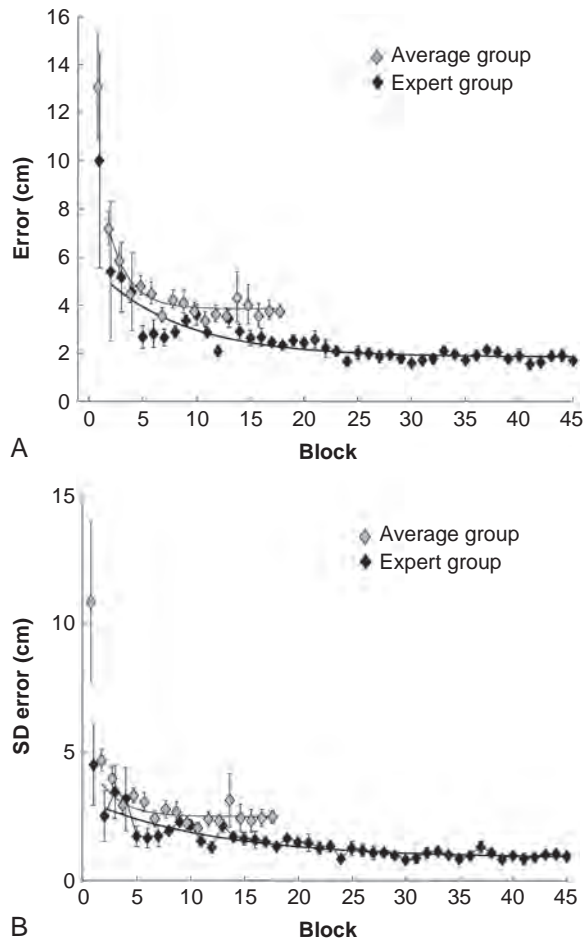


Figure 12.5 Changes in the error to the target with practice. For each block, the data of 60 trials were averaged. Participants performed three blocks of trials per day. **A:** Mean error for 12 participants over 18 blocks (6 days) of practice are shown in gray. Results for the expert participants over 45 blocks (15 days) of practice are shown in black. Error bars show standard error across participants. **B:** Standard deviations of error averaged over participants across blocks of trials. Error bars show standard error across participants.

- 1 more tightly clustered—*Noise* was reduced, and the data displayed even
- 2 more pronounced *Covariation*.
- 3 Numerical estimates of the three costs were calculated for each partici-
- 4 pant for each block of 60 trials, hence rendering three estimates per day.
- 5 Note the cost estimate is interpretable and expresses how much the average
- 6 error could be reduced if this particular cost were minimized. The
- 7 results of the three costs are therefore directly comparable. It should be

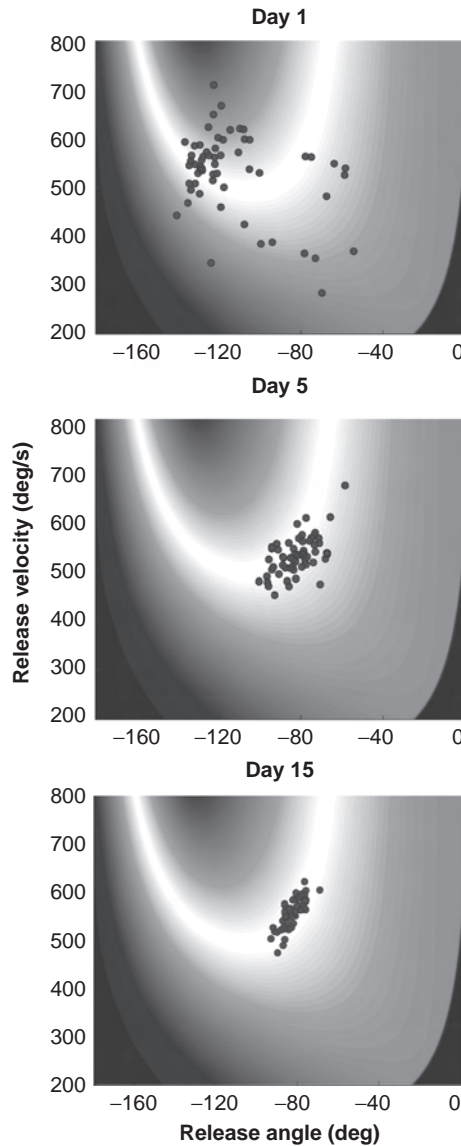


Figure 12.6 Representative example of improvement of skittle tasks over 15 days of practice. Data of one expert subject is plotted in execution space.

1 pointed out, though, that the three costs do not sum to the total error in
 2 performance. Typically, their sum is higher than the average error as the
 3 components are not exclusive and independent. Most notably, $T\text{-Cost}$ of a
 4 particular data set depends on its $N\text{-Cost}$: The strategy depends on the
 5 overall dispersion of the data. Data with very little dispersion do not require

1 a very error-tolerant strategy. This interrelation is interesting and has
 2 potential for further exploration. Could it be that, for people who have
 3 large variability, as for example due to tremor or other neurological disor-
 4 ders, different movement strategies are appropriate? Conversely, if people
 5 have low variability, then many more strategies are available. According to
 6 this logic, manipulation of variability may be a way to influence movement
 7 strategies.

8 Figure 12.7 shows the mean results of the three costs for both participant
 9 groups together with their exponential fits; the error bars denote standard
 10 error across participants. The time profiles are similar for both experts and
 11 average subjects: *T-Cost* shows a sharp decline early in practice, *C-Cost* and
 12 *N-Cost* have a slower decline over time with similar time constants; how-
 13 ever, note the different scale on the y-axis of *C-Cost* and *N-Cost*.

14 Hence, plotting the fitted exponential curves in a single graph in
 15 Figure 12.8 permits better comparison of the three costs. Inspecting the pro-
 16 files for the average group and the three expert individuals together reveals
 17 that the rank ordering of the three costs is consistent for all participants.
 18 *T-Cost* either drops sharply in the very beginning or is already exploited,
 19 leaving little room for improvement. Interestingly, *N-Cost* is the highest
 20 and also remains highest. The three expert individuals show that only after
 21 many days of practice does *N-Cost* approach similar levels as *C-Cost*.

22 These results are nontrivial, as they show that *Noise* is highest and the
 23 last component to be decreased. Considering that many studies on motor
 24 learning have reported decreases in variability with practice as the typical
 25 signature of skill, this decomposition suggests a new interpretation of this
 26 ubiquitous finding. Although the decrease of variability in error measures
 27 was typically quantified by standard deviations and interpreted as a change
 28 in random noise, the TNC-decomposition suggests that more systematic
 29 aspects of variability are responsible for the observed decrease. In the
 30 beginning are changes of strategy, in which subjects explore and find new
 31 ways of executing the task. This is followed by optimizing covariation in
 32 alignment with the solution manifold (i.e., existent variability in execution
 33 is channeled into “do-not-care-directions”). Only very late in practice does
 34 the noise component experience an improvement. It can be concluded that
 35 the fluctuations that remain present even after long practice are truly
 36 random elements.

37 The notion of channeling variability into do-not-care-directions is close
 38 to what the analysis approach of the UCM approach (Latash, Scholz, and
 39 Schöner, 2002) extracts from data and is also implicit in the OFC frame-
 40 work (Todorov and Jordan 2002; Todorov 2004). Hence, some discussion of
 41 both approaches is warranted. Before doing so, however, it should be
 42 emphasized that the present model task has redundancy in state space
 43 defined by angle and velocity at execution. As the two dimensions have
 44 different units, the space has no distance measure and does not permit the
 45 application of covariance-based analysis. The UCM and OFC approaches are

AQ? Latash,
 Scholz, and Schöner,
 2002 is not in ref list

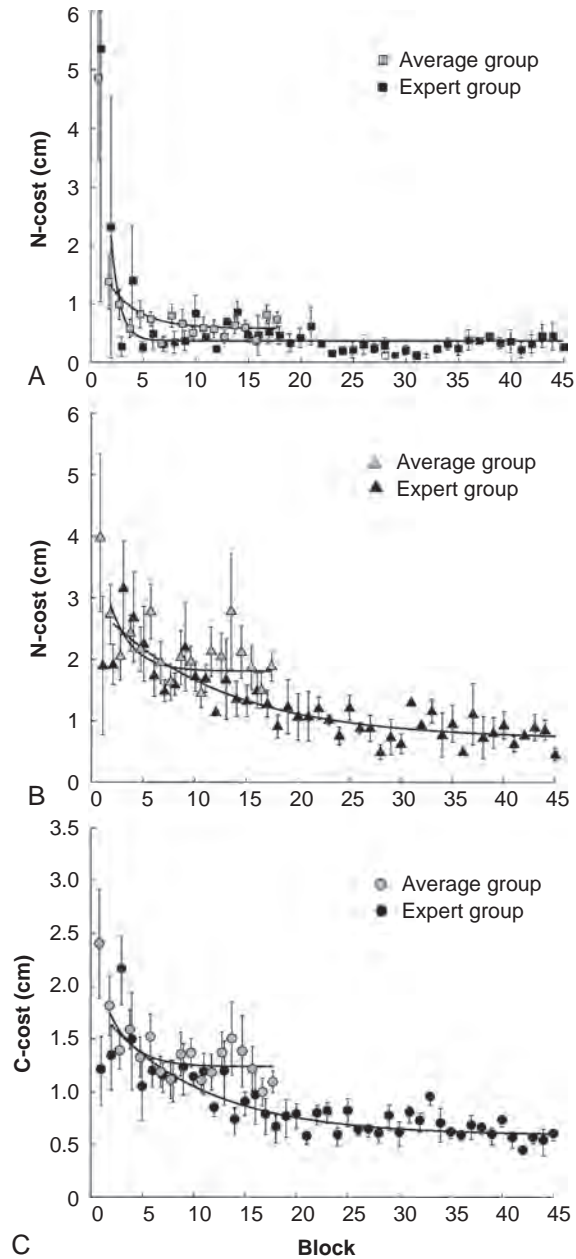


Figure 12.7 Changes in *T-Cost*, *N-Cost* and *C-Cost* over practice. Mean results for 12 participants over 18 blocks (6 days) of practice are shown as in gray. Results for the expert group over 45 blocks (15 days) of practice are shown in black. Error bars show standard error across participants.

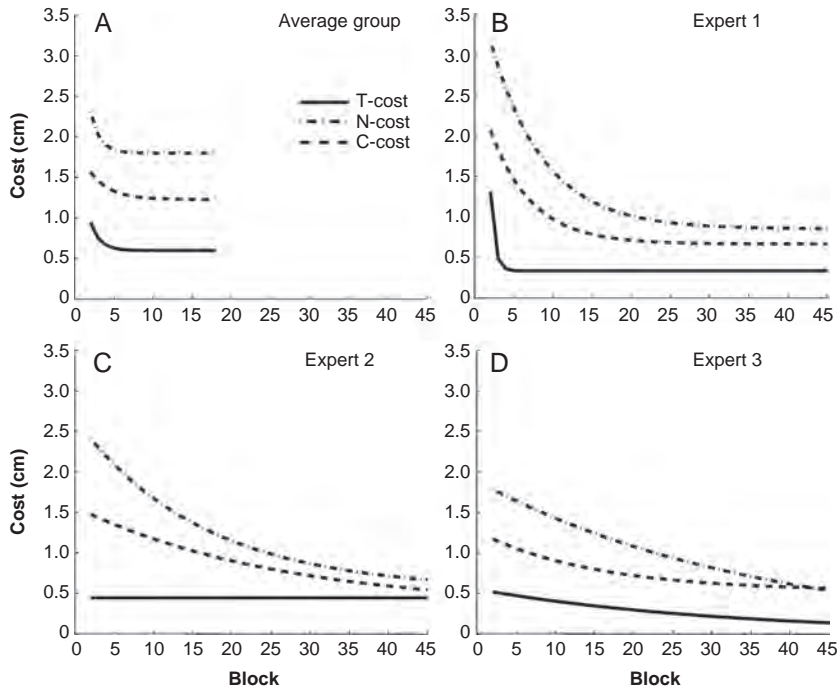


Figure 12.8 Exponential fits to *T-Cost*, *N-Cost*, and *C-Cost* for the average and the expert group data. **A**: Exponential fits to the three costs for the group. **B–D**: Exponential fits for the three expert participants.

1 based on the analysis of the covariance matrix, similar to many other analy-
 2 ses of the structure of variability, such as principal component analysis and
 3 variants of independent component analysis. Hence, orthogonality—the key
 4 concept used to apply covariance-based analyses in motor experiments—
 5 cannot be meaningfully applied to this task (Schöner and Scholz 2007;
 6 Müller and Sternad 2009; Sternad et al. accepted). A significant difference
 7 of the TCN approach is that it analyzes variability not in the space of the
 8 execution variables, but in the space of the result or task outcome. The
 9 important consequence is that the TCN analysis does not require a mean-
 10 ingful definition of distance in execution space.

11 Putting the issue of metrics aside, another distinct aspect of the TNC
 12 method is its parsing of variability into three components. In comparison,
 13 UCM distinguishes between variability parallel and orthogonal to the
 14 manifold. These correspond to covariation or the lack thereof in the TNC
 15 approach. Changes in the magnitude of the dispersion are not separated
 16 from changes in the anisotropy of the variability. That said, such an exten-
 17 sion could be relatively straightforward. An additional conceptual differ-
 18 ence is that the UCM analysis assumes that the system is at its best location.

1 In the TNC approach, the quantification of the best location that offers
 2 stability—*Tolerance*—compared to the actual location, is new and distinct.
 3 This aspect pays tribute to the fact that, in order to find the best strategy,
 4 variability is required that reveals information about where this strategy is:
 5 Variability or *Noise* presents an opportunity to learn and improve.

6 Sensitivity to Intrinsic Variability: Optimizing Tolerance

7 To what degree are subjects aware of their intrinsic noise and seek move-
 8 ment strategies that are tolerant to this noise? As introduced earlier in
 9 Figure 12.1, stability in both continuous and discrete dynamical systems is
 10 tightly intertwined with the noise intrinsic to the system. Hence, it is rea-
 11 sonable to expect that actors are aware of their inherent variability when
 12 executing a movement. However, the magnitude of this noise is not neces-
 13 sarily constant, and it is reasonable to assume that it is varying. One well-
 14 known determinant of the magnitude of noise is the velocity or force with
 15 which a movement is executed. The level of noise is a function of the mag-
 16 nitude of the signal. Such signal-dependent noise has been observed in
 17 many different motor tasks, ranging from isometric force production to
 18 rhythmic interval production, and is also conceptually consistent with
 19 Weber's Law (Worringham 1991; 1993; Ivry and Hazeltine 1995; Slifkin and
 20 Newell 1999).

21 Given such varying noise, how do actors plan their actions? Do they
 22 seek out the most noise-tolerant strategies as defined by the task? Or, are
 23 they aware of determinants such as velocity-dependent noise in their exe-
 24 cution and therefore minimize their movement velocity? The costs arising
 25 from a nonoptimal movement strategy—especially *Tolerance* or *T-Cost*—
 26 can be extracted not only post hoc from the data, but can also be predicted
 27 for a given task. If the physics of the experimental task is known—as in the
 28 skittles task—stable or error-tolerant executions can be identified if a given
 29 amount of noise is assumed. Two experiments were designed to derive
 30 such predictions about tolerant solutions and to test the hypothesis that
 31 subjects seek solutions that minimize the effect of this variability on their
 32 performance result (Sternad et al. under revision).

33 *Hypotheses and Execution Space*

34 Three specific hypotheses were contrasted: *Hypothesis 1* states that subjects
 35 prefer those strategies that have the highest *Tolerance* or least *T-Cost*.
 36 Predictions of expected performance were calculated based on estimates
 37 of subjects' variability. The first hypothesis assumed constant levels of
 38 noise for all possible executions. If one takes into account that higher move-
 39 ment velocities are typically accompanied by higher variability, then it can
 40 be expected that solutions with high release velocities are avoided.
 41 Therefore, *Hypothesis 2* posits that subjects chose solutions with the lowest

1 possible velocities. This hypothesis is also supported by the argument that
2 lower velocities present more energy-efficient solutions. In the skittles task,
3 these two hypotheses can make contrasting predictions when the most
4 error-tolerant solution is not at the location with minimum velocity. Given
5 that both criteria may compete with each other, *Hypothesis 3* posits that
6 subjects chose solutions that trade-off between error-tolerance and low
7 velocity-dependent noise.

8 To test the three hypotheses, the task was manipulated to create two
9 different execution spaces by changing the location of the target skittle and
10 the center post. Figure 12.9A illustrates the configuration of target and post
11 in the workspace and the associated execution space and result function
12 in Figure 12.9B for the first experiment. The locations of target and post
13 were designed so as to achieve a result function with a very different cur-
14 vature adjacent to the solution manifold (i.e., different levels of *Tolerance*).
15 Successful solutions were relatively insensitive to release angle; that is,
16 approximately parallel to the x-axis; the most error-tolerant location was at
17 angle -0.7 rad and velocity 3 rad/s. Although this solution offered both
18 error-tolerance at low velocities, solutions in this vicinity were “risky”
19 (i.e., close to the post hits that are penalized heavily). The configuration of
20 the second experiment, illustrated in Figure 12.9C and D, created a conflict
21 between optimal solutions with respect to *Tolerance* and minimization of
22 velocity. The most error-tolerant solution was at an angle of 1.5 rad, with
23 *Tolerance* increasing only slightly, but monotonically with increasing veloc-
24 ity. The solution with the lowest velocity was adjacent to post hits and
25 therefore again posed a risky strategy. If actors were aware of their intrinsic
26 noise, a useful strategy for execution would be one that either had the
27 lowest successful velocity or one that had slightly higher velocities but
28 better *Tolerance*.

29 In the first experiment, nine subjects performed three sessions, each con-
30 sisting of 180 trials, yielding a total of 540 trials; in the second experiment,
31 nine different subjects performed five sessions, giving a total of 900 trials.
32 In session 1 of both experiments, participants were instructed to try differ-
33 ent release angles and release velocities to find successful strategies that
34 achieved reliable solutions. In the subsequent sessions, participants were
35 instructed to no longer explore but to continue with the strategy that had
36 proven most successful. They were encouraged to fine-tune their perfor-
37 mance and avoid hitting the center post, as they would receive a large
38 penalty.

39 To quantitatively test the three hypotheses, the expected performance
40 for each location in execution space, $E(P)$ was calculated as the average
41 distance error d in a neighborhood around a location (α_i, v_j) ; the size of the
42 neighborhood captured the subject’s variability. To calculate $E(P)$, the exe-
43 cution space was divided into 360×360 bins and $E(P)$ was determined for
44 each (α_i, v_j) , with $i, j = 1, 2, \dots, 360$. Before these calculations, the individual

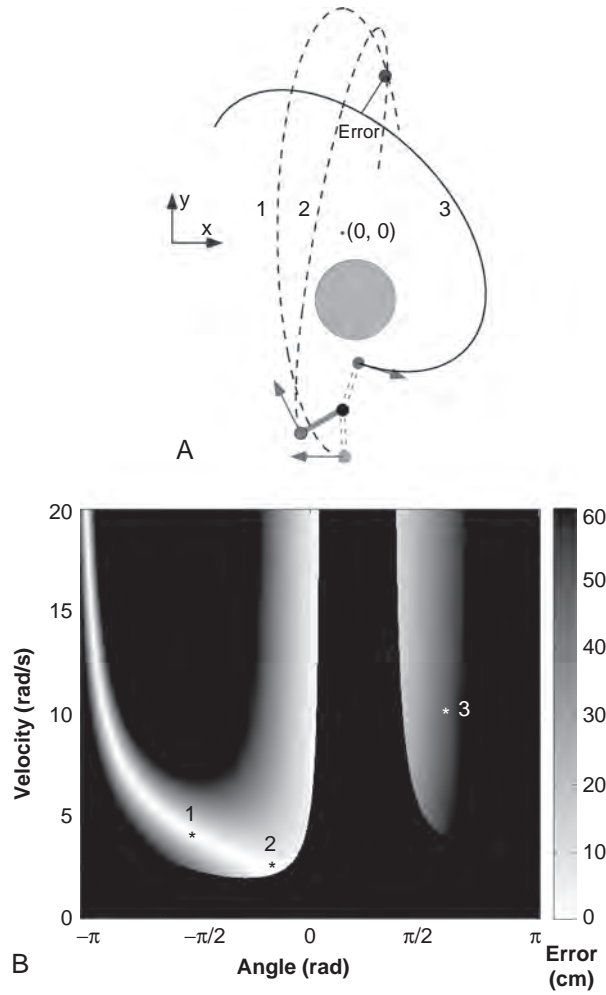


Figure 12.9 Workspace, execution space, and solution manifold. **A:** Workspace with the position of the center post and target of Experiment 1. Two ball trajectories exemplify how different release variables can lead to the same result with zero error, $d = 0$ (trajectory 1, 2, *dashed line*). Trajectory 3 shows a trajectory with non-zero error, $d = 30$ cm. **B:** Execution space and solution manifold. White denotes zero-error solutions, increasing error is shown by increasingly darker gray shades, black denotes a post hit. The release variables of trajectory 1 and 2 correspond to points 1, 2 on the solution manifold, the variables of trajectory 3 correspond to the point 3 in a gray-shaded area.

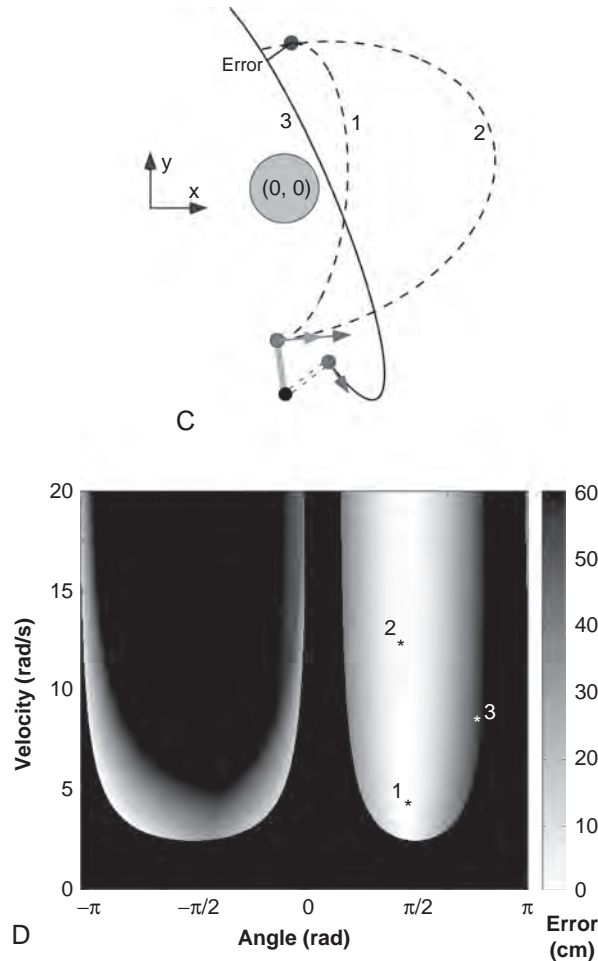


Figure 12.9 (Continued) C: Workspace with center post and target as used in Experiment 2. Three select trajectories exemplify the redundancy of solutions. D: Corresponding execution space and solution manifold. The three points correspond to the three trajectories of panel C.

AQ? Is something missing from this equation?

- 1 result or error values $d(\alpha_i, v_j)$ were transformed from a penalty function
- 2 into a reward function $P(\alpha_i, v_j)$:

- 3
$$P(\alpha_i, v_j) = |d(\alpha_i, v_j) - 60 \text{ cm}|$$

- 4 where 60 cm was the initially assigned post hit.
- 5 For each execution, (α_i, v_j) a matrix with Gaussian weights was defined.
- 6 The size of the matrix was calculated from the actual standard deviations

1 of angle and velocity, SDa , SDv , determined post hoc from all nine partici-
 2 pants. This yielded a matrix of 15 ($a, k = -7$ to 7) \times 23 ($v, n = -11$ to 11) cells
 3 with the probability distribution $p(\alpha_{i+k}, v_{j+n})$:

$$p(\alpha_{i+k}, v_{j+n}) = pdf\left(\frac{\alpha_i - \alpha_{i+k}}{SD\alpha}\right) * pdf\left(\frac{v_j - v_{j+n}}{SDv}\right), \quad (\text{Eq. 2})$$

4 where pdf is the probability density function of the bivariate normal
 5 distribution with mean (α_i, v_j) and standard deviations (SDa , SDv). The
 6 expected performance $E(P_{ij})$ at (α_i, v_j) was defined as
 7

$$E(P_{ij}) = E(P(\alpha_i, v_j)) = \sum_{k=-7}^7 \sum_{n=-11}^{11} p(\alpha_{i+k}, v_{j+n}) * P(\alpha_{i+k}, v_{j+n}) \quad (\text{Eq. 3})$$

8 Finally, all $E(P_{ij})$ values were normalized, dividing by the largest value
 9 to confine them to the interval between 0 and 1.

10 For the first experiment, the predictions for Hypothesis 1 are illustrated
 11 in Figure 12.10A: expected performance $E(P)$ was highest at $a = -0.7$ rad
 12 and $v = 3.0$ rad/s, defining the most error-tolerant solution. This optimum
 13 is approximately coincident with what is predicted by Hypothesis 2—where
 14 velocity is at a minimum (not shown separately). For the target constella-
 15 tion of the second experiment, the $E(P)$ values for Hypothesis 1 are illus-
 16 trated in Figure 12.10B. Importantly, the maximum $E(P)$ and highest
 17 *Tolerance* was coincident with the highest velocity. In contrast, Hypothesis 2
 18 predicted solutions at the lowest velocity at 3.1 rad/s and the invariant
 19 angle of 1.4 rad. The trade-off between maximizing error-tolerance and
 20 minimizing velocity, as posited in Hypothesis 3, was calculated with
 21 the size of the probability matrix scaled proportionally to velocity: larger
 22 sizes at higher velocities were expected from velocity-dependent noise.
 23 Hypothesis 3 is visualized in Figure 12.10C. The maximum value of $E(P)$
 24 was at $a = 1.4$ rad and $v = 7.5$ rad/s.

25 The pooled results from all nine participants in the first experiment is
 26 shown in Figure 12.11A. The histogram pools all trials and presents the
 27 data on a grid of 36×36 bins. (As the focus was on solutions that partici-
 28 pants had reached after some exploration, the first practice session was
 29 discarded from analysis.) The distribution was clearly nonuniform and
 30 clustered around a mode at -0.73 rad and 2.65 rad/s. This mode was close
 31 to the optimal $E(P)$ as predicted by Hypothesis 1 (-0.70 rad, 3.0 rad/s). Note
 32 that the highest frequency of trials was also close to the locations with the
 33 high penalty; that is, executions that lead to a post hit (shown in black).

34 For statistical testing, these two-dimensional data were collapsed into
 35 36 bins of the angle dimension. The same procedure was followed for the
 36 predicted $E(P)$ values. Figure 12.11B shows both the data and the $E(P)$
 37 values as predicted by Hypothesis 1 and 2. The Spearman rank correlations
 38 between data and each of the two hypotheses were highly significant. This
 39 provided support that subjects preferred solutions with highest tolerance
 40 and lowest velocities, even though these solutions were risky.

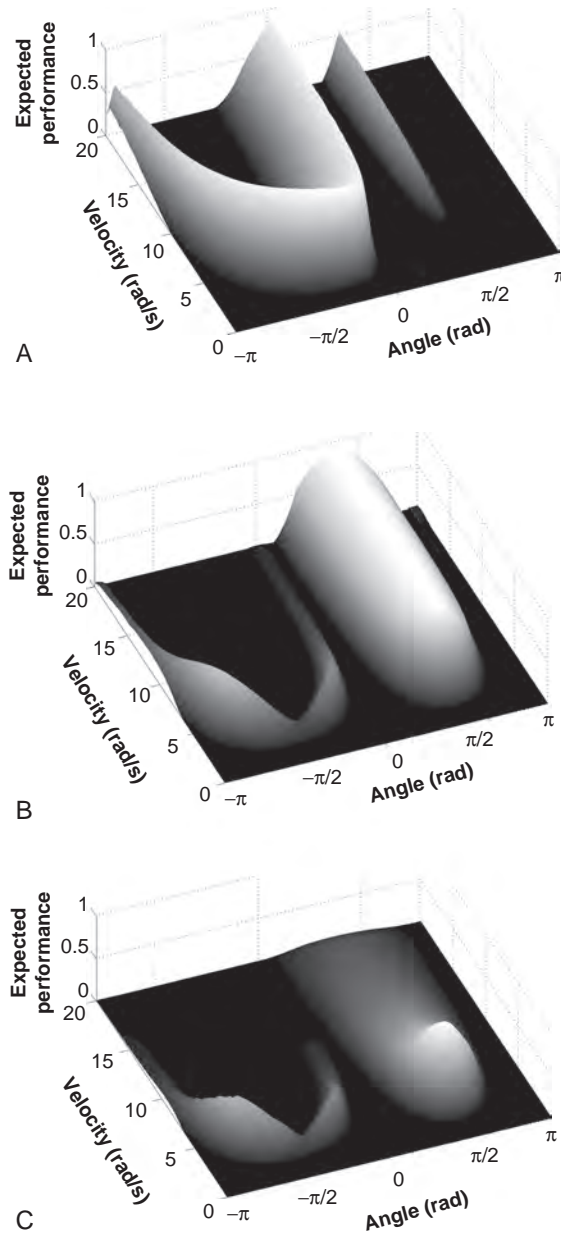


Figure 12.10 Simulation of hypotheses. **A:** Simulation of hypothesis 1 for Experiment 1: The vertical dimension represents expected performance $E(P)$, which are average values calculated from a Gaussian-weighted matrix of execution variables. The most error-tolerant solution with maximum $E(P)$ is at $-\pi/2$ rad and 3 rad/s. **B:** Simulation of hypothesis 1 for Experiment 2. Expected performance $E(P)$ at an angle of approximately 1.4 rad is similarly high across the entire range of velocity. **C:** Simulation of hypothesis 3 for Experiment 2. The expected performance $E(P)$ decreases for higher velocity due to the simulated velocity-dependent noise. Maximum $E(P)$ is at an angle of 1.4 rad with a velocity of 7.5 rad/s.

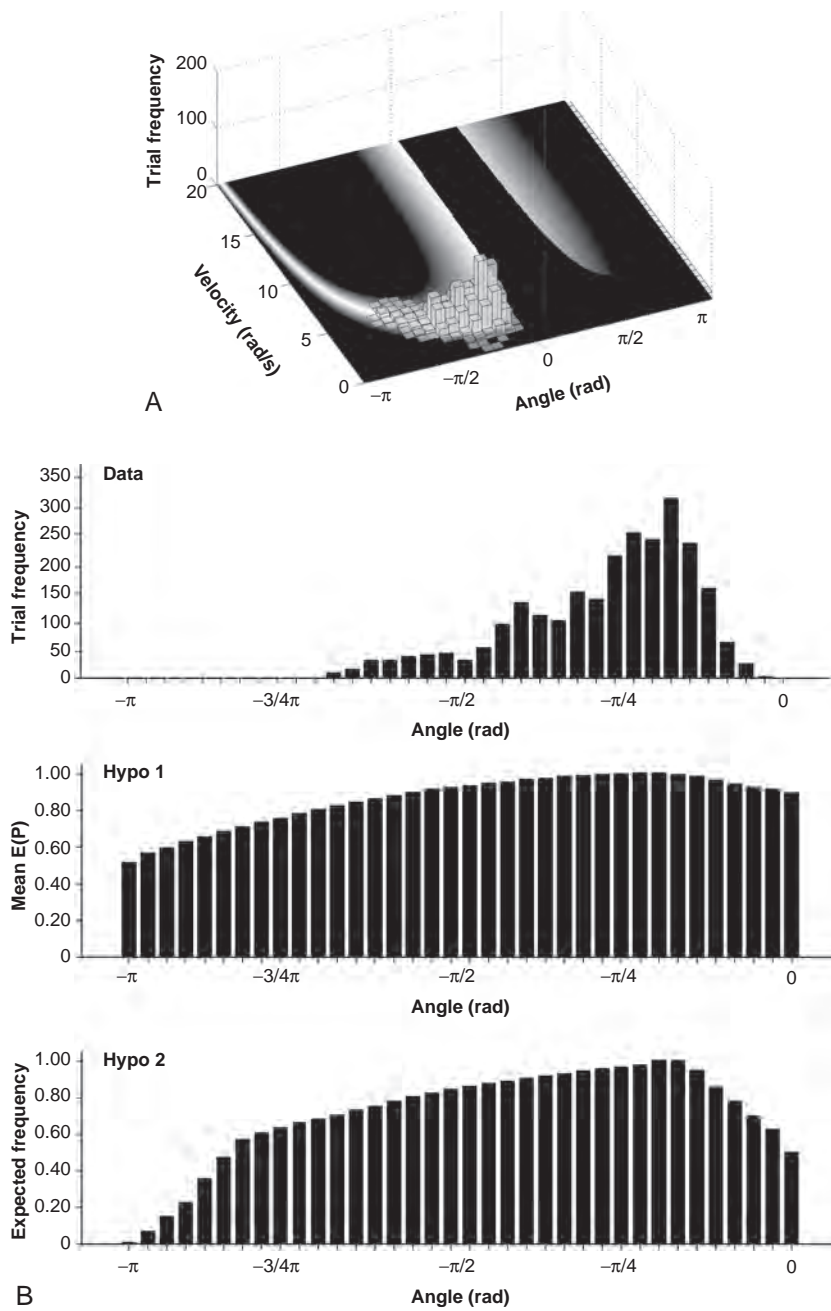


Figure 12.11 Result of Experiment 1. **A:** Histogram of all subjects' trials plotted in execution space; the mode of the two-dimensional distribution is close to the predicted location with maximum expected performance $E(P)$. **B:** Histograms in the angular dimension: Top panel shows the data distribution; middle panel shows the predicted distributions $E(P)$ of Hypothesis 1; bottom panel shows the expected frequency $E(F)$ of Hypothesis 2.

1 The results of the second experiment are shown in Figure 12.12A. The
 2 histogram in execution space pools all trials of all participants in sessions
 3 2 to 5 onto a grid of 36×36 . The data were distributed across a large range
 4 of velocities between 2.5 and 15.3 rad/s. To test the hypotheses, the data
 5 and the hypothesized $E(P)$ distributions from the three hypotheses were
 6 collapsed onto the velocity dimensions (Fig. 12.12B). Spearman correlation
 7 tests showed that the correlation between data and Hypothesis 3 was
 8 significant, whereas the data did not correlate with predictions from
 9 Hypotheses 1 and 2.

10 Overall, the results of the two experiments gave support to the hypoth-
 11 esis that subjects are aware (not necessarily consciously) of their variability
 12 and choose those solutions that are either more tolerant to noise or have
 13 less noise associated with it. In previous work, it has been shown that vari-
 14 ability scales with movement speed, such that performance at higher veloci-
 15 ties is more variable (Schmidt et al. 1979; Worringham 1991; 1993).
 16 Assuming movement velocity reflects a magnitude of the motor control
 17 signal, this observation is consistent with variability increasing with signal
 18 strength (Harris and Wolpert 1998). Physiologically, this behavioral obser-
 19 vation has been related to the organizational properties of the motor unit
 20 pool, such as recruitment order and twitch amplitudes (Jones et al. 2002;
 21 Hamilton et al. 2004). Even though these muscle–physiological studies
 22 focused on isometric contractions, it can be generalized to movements with
 23 high velocities as higher velocities require higher and faster rates of muscle
 24 contractions.

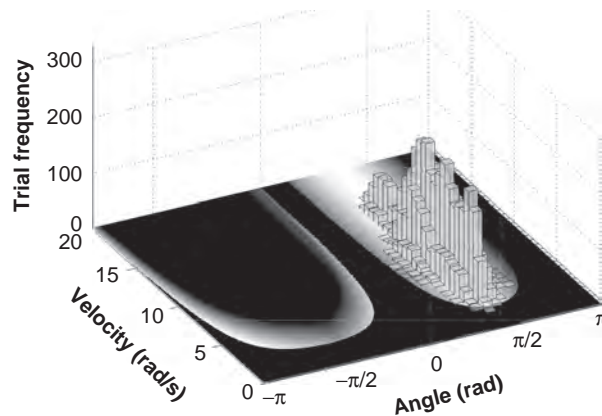


Figure 12.12 Result of Experiment 2. A: Histogram of all subjects' trials of four sessions plotted in execution space (720 trials per subject). The distribution is spread along a long range of velocities from 2.5 and 15.3 rad/s at an angle of 1.4 rad.

12. Variability, Noise, and Sensitivity to Error

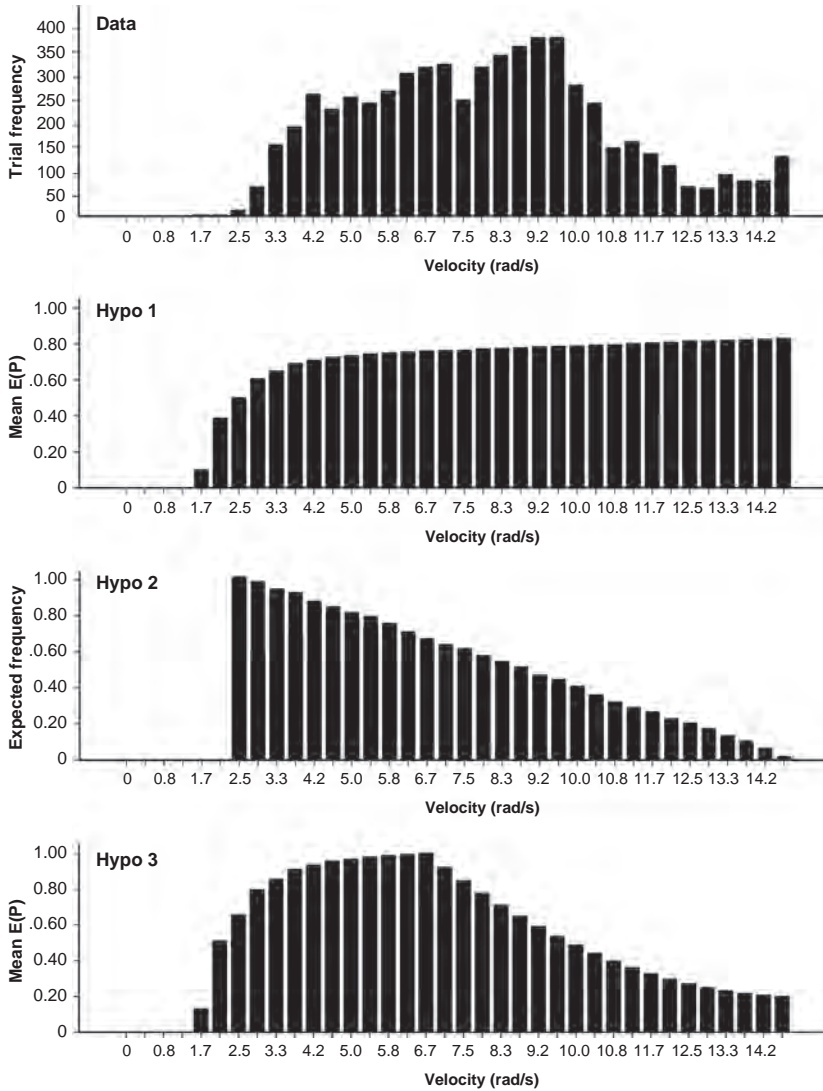


Figure 12.2 (Continued) B: Projection of the distributions to the velocity dimension. The top panel shows the data; the three panels below show the predicted distributions of Hypothesis 1, 2, and 3.

1 To test this alternative explanation, the second experiment was designed
2 to distinguish between the two alternative hypotheses and test the third
3 hypothesis that both criteria are of equal relevance. Indeed, subjects were
4 shown to seek the optimum between the two sources of variability. Such a
5 trade-off between signal dependent-noise and instability in an isometric
6 force production task has recently been shown by Selen and colleagues
7 (Selen et al. 2009).

8 Tolerance, Sensitivity Analysis, and Decision Theory

9 The influence of noise in learning movement strategies was investigated by
10 simulations that tested the sensitivity of solutions to noise. Analysis
11 of robustness and sensitivity is common, but our approach differs from
12 standard sensitivity analyses as it includes variability in an extended neigh-
13 borhood around each solution. Local linear stability analysis assesses the
14 effect of small deviations from a single solution, typically, the fixed-point
15 solution of a dynamical system. Relaxation time provides a quantitative
16 measure for how fast a system returns to the stable solution; the faster
17 the return, the more attractive and stable the system. This linear approach
18 is ignorant to the effects of slightly larger errors. Knowledge of errors in
19 an extended neighborhood of the stable solution, however, is important
20 when the system is nonlinear and has discontinuities. In the skittles task,
21 the result variable is a nonlinear function of the execution variables with
22 discontinuities; hence, such an approach is warranted. Additionally, con-
23 sidering that in human performance perturbations or errors are not infini-
24 tesimally small but rather have a sizable variance, it is appropriate to assess
25 error sensitivity not only at a point, but in a neighborhood around a chosen
26 solution.

27 The rationale of the present analysis is in overall accordance with deci-
28 sion theory as applied in a series of experiments by Trommershäuser
29 and colleagues (Trommershäuser et al. 2003; Trommershäuser et al. 2005).
30 The calculations for expected performance $E(P)$ are equivalent to calculat-
31 ing expected utility, with $P(\alpha, \nu)$ representing the utility or cost function
32 (Berger 1985; Trommershäuser et al. 2003). Their studies used a speed-
33 accuracy instruction, in which the target of a pointing task was bounded
34 by a penalty area, and the distribution of hits was examined with respect to
35 the relative position of target and penalty area. The gain function had
36 an optimum defined by the weighted sum of the gain and the subject's
37 inherent variability. The results showed systematic effects of the penalty on
38 the data distributions and, similar to our work, supported that selection
39 of a movement strategy was determined by the subject's inherent variabil-
40 ity. However, the study also differed from our skittles task in that hitting
41 success was binary (positive for the target area and negative for the penalty
42 area). In contrast, our task permitted to estimate the continuous distance

1 to the target, which was prerequisite to the sensitivity analysis in our
2 study.

3 **A Task with a Hidden Layer**

4 The skittles task differs in one further important aspect to Trommershäuser's
5 experiments: in the pointing task, the reward or penalty was directly visi-
6 ble to the subject. Hence, it is relatively straightforward in that subjects
7 avoid the visible penalty area. In contrast, in the skittles task, the penalty or
8 high-reward areas are sets of release parameters that are not visible. Rather,
9 subjects have to explore the "landscape" of the task with their actions and
10 learn the "location" of the solution manifold. This more indirect nature of
11 the task is noticeable when we had children perform the task. Surprisingly,
12 this "hidden layer" of the task posed severe problems to children of young
13 age, and their typical learning patterns differed significantly from adult
14 subjects. Children seemed to have a larger initial barrier to explore differ-
15 ent solutions if their first attempts were not successful. Despite lack of suc-
16 cess, they adhered more strongly to their preferred release value (Chu et al.
17 2009). In addition, their arm and ball trajectories were more stereotypical,
18 even though the variability in the result error was caused by larger vari-
19 ance in release time along a relatively invariant trajectory. These observa-
20 tions indicated that, compared to adults, children were less able to use
21 flexible search strategies and could not discover or infer the hidden
22 nonlinear mapping between execution variables and the result. These dif-
23 ferences highlight developmental changes in motor learning strategies
24 (Chu et al. 2009). Hence, tasks with hidden layers pose interesting new
25 problems for understanding processes underlying motor learning.

26 **CONCLUSION**

27 The reviewed findings lay the foundations for a number of new investiga-
28 tions. Ongoing work uses the TCN framework to assess performance of
29 subjects with neurological impairments, such as Parkinson patients and
30 children with cerebral palsy. The evident next step is to develop interven-
31 tion techniques that influence *Tolerance*, *Covariation*, and *Noise* and thereby
32 facilitate and guide skill learning and also recovery.

33 **ACKNOWLEDGMENTS**

34 This research was supported by grants from the National Science
35 Foundation, BCS-0450218, the National Institutes of Health, R01-HD045639,
36 and the Office of Naval Research, N00014-05-1-0844. We would like to
37 express our thanks to Hermann Müller, Tjeerd Dijkstra, and Neville Hogan
38 for many insightful discussions. We would also like to express our thanks

1 to Virginia Chu and Terry Sanger and the members of the Action Lab, who
 2 all contributed to these experiments: Kunlin Wei, Rajal Cohen, Xiaogang
 3 Hu, and Lisa Pendt.

4 REFERENCES

- 5 Berger, J.O. 1985. *Statistical decision theory and Bayesian analysis*, 2nd edition.
 6 New York: Springer.
- 7 Chu, V.W.T., D. Sternad, and T.D. Sanger. 2009. Learning a redundant task in adults
 8 and children. *Society for Neuroscience Abstracts* 369–27.
- 9 Churchland, M.M., A. Afshar, and K.V. Shenoy. 2006. A central source of movement
 10 variability. *Neuron* 52:1085–96.
- 11 Cohen, R.G., and D. Sternad. 2009. Variability in motor learning: Relocating, chan-
 12 neling and reducing noise. *Experimental Brain Research* 193:69–83.
- 13 Craig, J.J. 1986. *Introduction to robotics*. Reading, MA: Addison-Wesley.
- 14 Faisal, A.A., L.P. Selen, and D.M. Wolpert. 2008. Noise in the nervous system. *Nature*
 15 *Reviews. Neuroscience* 9:292–303.
- 16 Gel'fand, I.M., and M.L. Tsetlin. 1962. Some methods of control for complex
 17 systems. *Mathematical Surveys* 17:95–116.
- 18 Gordon, J., M.F. Ghilardi, and C. Ghez. 1994. Accuracy of planar reaching move-
 19 ments. I. Independence of direction and extent variability. *Experimental Brain*
 20 *Research* 99:97–111.
- 21 Hamilton, A.F., K.E. Jones, and D.M. Wolpert. 2004. The scaling of motor noise with
 22 muscle strength and motor unit number in humans. *Experimental Brain*
 23 *Research* 157:417–30.
- 24 Harris, C.M., and D.M. Wolpert. 1998. Signal-dependent noise determines motor
 25 planning. *Nature* 394:780–84.
- 26 Hore, J., D. Timmann, and S. Watts. 2002. Disorders in timing and force of finger
 27 opening in overarm throws made by cerebellar subjects. *Annals of the*
 28 *New York Academy of Sciences* 978:1–15.
- 29 Ivry, R.B., and R.E. Hazeltine. 1995. Perception and production of temporal
 30 intervals across a range of durations: Evidence for a common timing mecha-
 31 nism. *Journal of Experimental Psychology. Human Perception and Performance*
 32 21:3–18.
- 33 Jones, K.E., A.F. Hamilton, and D.M. Wolpert. 2002. Sources of signal-dependent
 34 noise during isometric force production. *Journal of Neurophysiology* 88:
 35 1533–44.
- 36 Körding, K.P., S.P. Ku, and D.M. Wolpert. 2004. Bayesian integration in force esti-
 37 mation. *Journal of Neurophysiology* 92:3161–65.
- 38 Körding, K.P., and D.M. Wolpert. 2004. Bayesian integration in sensorimotor learn-
 39 ing. *Nature* 427:244–47.
- 40 Latash, M.L. 2008. *Synergy*. Oxford: Oxford University Press.
- 41 Latash, M.L., Scholz, J.P., and G. Schöner. 2002. Motor control strategies revealed
 42 in the structure of motor variability. *Exercise and Sport Sciences Reviews* 30:
 43 26–31.
- 44 Liu, D., and E. Todorov. 2007. Evidence for the flexible sensorimotor strategies
 45 predicted by optimal feedback control. *Journal of Neuroscience* 27:9354–68.
- 46 Martin, T.A., B.E. Greger, S.A. Norris, and W.T. Thach. 2001. Throwing accuracy in
 47 the vertical direction during prism adaptation: Not simply timing of ball
 48 release. *Journal of Neurophysiology* 85:2298–302.
- 49 Miyazaki, M., D. Nozaki, and Y. Nakajima. 2005. Testing Bayesian models of human
 50 coincidence timing. *Journal of Neurophysiology* 94:395–99.

- 1 Müller, H., and D. Sternad. 2004. Decomposition of variability in the execution of
2 goal-oriented tasks - Three components of skill improvement. *Journal of*
3 *Experimental Psychology: Human Perception and Performance*, 30: 212–233.
- 4 Müller, H., and D. Sternad. 2009. Motor learning: Changes in the structure of vari-
5 ability in a redundant task. *Advances in Experimental Medicine and Biology*
6 629:439–56.
- 7 Osborne, L.C., S.G. Lisberger, and W. Bialek. 2005. A sensory source for motor
8 variation. *Nature* 437:412–16.
- 9 Schmidt, R.A., and T. Lee. 2005. *Motor control and learning: A behavioral emphasis*, 4th
10 edition. Champaign, IL: Human Kinetics.
- 11 Schmidt, R.A., H. Zelaznik, B. Hawkins, J.S. Frank, and J.T., Quinn Jr. 1979. Motor-
12 output variability: A theory for the accuracy of rapid motor acts. *Psychological*
13 *Review* 47:415–51.
- 14 Scholz, J.P., and G. Schöner. 1999. The uncontrolled manifold concept: Identifying
15 control variables for a functional task. *Experimental Brain Research* 126:289–306.
- 16 Schöner, G., and J.P. Scholz. 2007. Analyzing variance in multi-degree-of-freedom
17 movements: Uncovering structure versus extracting correlations. *Motor Con-*
18 *trol* 11:259–75.
- 19 Selen, L.P., D.W. Franklin, and D.M. Wolpert. 2009. Impedance control reduces
20 instability that arises from motor noise. *Journal of Neuroscience* 29:12606–16.
- 21 Slifkin, A.B., and K.M. Newell. 1999. Noise, information transmission, and force
22 variability. *Journal of Experimental Psychology. Human Perception and Perfor-*
23 *mance* 25:837–51.
- 24 Sternad, D., Abe, M. O., X. Hu, and H. Müller H. under revision. Neuromotor noise,
25 sensitivity to error and signal-dependent noise in trial-to-trial learning.
- 26 Sternad, D., H. Müller, S. Park, and N. Hogan. 2010. Coordinate dependency of
27 variability analysis. *PLoS Computational Biology* 6:e1000751.
- 28 Strogatz, S.H. 1994. *Nonlinear dynamics and chaos: With applications to physics, biology,*
29 *chemistry, and engineering*. Reading, MA: Perseus Books.
- 30 Timmann, D., R. Citron, S. Watts, and J. Hore. 2001. Increased variability in finger
31 position occurs throughout overarm throws made by cerebellar and unskilled
32 subjects. *Journal of Neurophysiology* 86:2690–702.
- 33 Todorov, E. 2004. Optimality principles in sensorimotor control. *Nature Neuroscience*
34 7:907–15.
- 35 Todorov, E. 2005. Stochastic optimal control and estimation methods adapted to
36 the noise characteristics of the sensorimotor system. *Neural Computation*
37 17:1084–108.
- 38 Todorov, E., and M.I. Jordan. 2002. Optimal feedback control as a theory of motor
39 coordination. *Nature Neuroscience* 5:1226–35.
- 40 Trommershäuser, J., S. Gepshtein, L.T. Maloney, M.S. Landy, and M.S. Banks. 2005.
41 Optimal compensation for changes in task-relevant movement variability.
42 *Journal of Neuroscience* 25:7169–78.
- 43 Trommershäuser, J., L.T. Maloney, and M.S. Landy. 2003. Statistical decision theory
44 and trade-offs in the control of motor response. *Spatial Vision* 16:255–75.
- 45 van Beers, R.J. 2009. Motor learning is optimally tuned to the properties of motor
46 noise. *Neuron* 63:406–17.
- 47 van Beers, R.J., P. Baraduc, and D.M. Wolpert. 2002. Role of uncertainty in senso-
48 rimotor control. *Philosophical Transactions of the Royal Society of London. Series*
49 *B, Biological Sciences* 357:1137–45.
- 50 van Beers, R.J., P. Haggard, and D.M. Wolpert. 2004. The role of execution noise in
51 movement variability. *Journal of Neurophysiology* 91:1050–63.
- 52 Wei, K., T.M. Dijkstra, and D. Sternad. 2007. Passive stability and active control in a
53 rhythmic task. *Journal of Neurophysiology* 98:2633–2646.

- 1 Wei, K., T.M. Dijkstra, and D. Sternad. 2008. Stability and variability: Indicators
- 2 for passive stability and active control in a rhythmic task. *Journal of Neuro-*
- 3 *physiology* 99:3027–41.
- 4 Worringham, C.J. 1991. Variability effects on the internal structure of rapid aiming
- 5 movements. *Journal of Motor Behavior* 23:75–85.
- 6 Worringham, C.J. 1993. *Predicting motor performance from variability measures.*
- 7 Champaign, IL: Human Kinetics.